Geophysical and geochemical signatures of Gulf of Mexico seafloor brines

S. B. Joye, I. R. Macdonald, J. P. Montoya, M. Peccini

Biogeosciences Discussions, 2, 637–671, 2005
www.biogeosciences.net/bgd/2/637/
SRef-ID: 1810-6285/bgd/2005-2-637
European Geosciences Union

Biogeosciences Discussions

Biogeosciences Discussions is the access reviewed discussion forum of *Biogeosciences*

Geophysical and geochemical signatures of Gulf of Mexico seafloor brines

S. B. Joye[1], I. R. MacDonald[2], J. P. Montoya[3], and M. Peccini[2]

[1]Department of Marine Sciences, University of Georgia, Athens, Georgia 30602, USA
[2]School of Physical and Life Sciences, Texas A&M University, Corpus Christi, Texas 78412, USA
[3]School of Biology, Georgia Institute of Technology, Atlanta, Georgia 30332, USA

Received: 21 April 2005 – Accepted: 3 May 2005 – Published: 31 May 2005

Correspondence to: S. B. Joye (mjoye@uga.edu)

Abstract

Geophysical, temperature, and discrete depth-stratified geochemical data illustrate differences between an actively venting mud volcano and a relatively quiescent brine pool in the Gulf of Mexico along the continental slope. Geophysical data, including laser-line scan mosaics and sub-bottom profiles, document the dynamic nature of both environments. Temperature profiles, obtained by lowering a CTD into the brine fluid, show that the venting brine was at least 10°C warmer than the bottom water. At the brine pool, two thermoclines were observed, one directly below the brine-seawater interface and a second about one meter below the first. At the mud volcano, substantial temperature variability was observed, with the core brine temperature being either slightly (~2°C in 1997) or substantially (19°C in 1998) elevated above bottom water temperature. Geochemical samples were obtained using a device called the "brine trapper" and concentrations of dissolved gases, major ions and nutrients were determined using standard techniques. Both brines contained about four times as much salt as seawater and steep concentration gradients of dissolved ions and nutrients versus brine depth were apparent. Differences in the concentrations of calcium, magnesium and potassium between the two brine fluids suggests that the fluids are derived from different sources or that brine-sediment reactions are more important at the mud volcano than the brine pool. Substantial concentrations of methane and ammonium were observed in both brines, suggesting that fluids expelled from deep ocean brines are important sources of methane and dissolved inorganic nitrogen to the surrounding environment.

1. Introduction

Submarine mud volcanoes are conspicuous examples of focused flow regimes in sedimentary settings (Carson and Screaton, 1998) and have been associated with high thermal gradients (Henry et al., 1996), shallow gas hydrates (Ginsburg et al., 1999), and an abundance of high-molecular weight hydrocarbons (Roberts and Carney, 1997).

BGD

2, 637–671, 2005

Mud volcanoes are common seafloor features along continental shelves, continental slopes, and in the deeper portions of inland seas (e.g. the Caspian Sea, Milkov, 2000) along both active and passive margins. Factors contributing to the formation of mud volcanoes include high sedimentation rates, tectonic activity, and tectonic compression (reviewed by Milkov, 2000). Along passive margins, mud volcanoes are associated with areas of rapid sedimentation (e.g. submarine fans such as the Niger Delta) or areas of high sedimentation combined with salt or shale tectonic activity (e.g. the Gulf of Mexico) (Milkov, 2000). Along active margins, mud volcanoes are associated with accretionary prisms (e.g. the Mediterranean Sea, Limonov et al., 1996; offshore Barbados, Lance et al., 1998; Langseth et al., 1988).

When salt diapers breach the sediment-water interface or extend to the shallow sub-bottom depths (<50 m; Reilly et al., 1996), brine-dominated seepage drives formation of brine-filled basins or smaller brine pools (Roberts and Carney ,1997). Brine-filled basins with diameters of several kilometers and depths of hundreds of meters are known from the Mediterranean Sea (Cita, 1990; Cita et al., 1989; De Lange and Brumsack, 1998; MEDINAUT/MEDINETH, 2000) and the outer continental slope of the Gulf of Mexico (Bouma and Bryant, 1994; MacDonald et al., 1990; Neurauter and Bryant, 1990; Neurauter and Roberts, 1994; Sheu, 1990; Shokes et al., 1977). Geochemical profiles through the seawater-brine interface in these basins show steep gradients in dissolved oxygen concentration, redox metabolites, temperature and salinity (Anschutz et al., 1998; Van Cappellen et al., 1998). Smaller brine-filled features form following rapid fluid expulsion, dissolution of shallow salt bodies, and/or the coalescence of salt diapirs and generate surface depressions that gradually fill with brine through lateral density flows (Bryant et al., 1990; Bryant et al., 1991; MacDonald et al., 1990; Roberts and Carney, 1997). These brine pools form a stable interface with seawater at the level of the crater rim (MacDonald et al., 1990). Sulfide-rich brines also occur as aquatanes at the base of deep-sea escarpments, for example on the western margin of the Florida platform (Commeau et al., 1987), where they are associated with abundant biomass of chemoautotrophic fauna.

Mud volcanoes, brine pools and brine basins are common in the Gulf of Mexico, an economically important hydrocarbon basin containing late Jurassic age oil and gas that was deposited in a diverse array of structural settings (Macgregor, 1993). The character of the Gulf of Mexico was shaped profoundly by the tectonics of a early Jurassic salt deposit (Pindell, 1985), which underlies the northwestern margin of the basin and has deformed and mobilized (Humphris, 1979) upward and to the south under the weight of Neogene sediments (Worrall and Snelson, 1989). Uplift or withdrawal of salt bodies creates diapirs or basins, respectively, that spawn irregular seafloor topography (Bryant et al., 1991) and fault networks that serve as conduits for the rapid transfer of brines, oil, and gas from deep reservoirs through the overlying sediments and ultimately into the water column (Kennicutt et al., 1988a, b; Aharon et al., 1992; Roberts and Carney, 1997). The association of dense chemoautotrophic-based communities with brine-dominated seeps has been documented in the Gulf of Mexico and elsewhere (e.g. Brooks et al., 1990; MacDonald et al., 1990; Milkov et al., 1996).

Brine-filled pools and basins contain a distinct volume of dense fluid retained below the level of the surrounding seafloor but in contact with the overlying seawater. Sampling the fluid from these often small, shallow basins and defining their morphology has been challenging. Here we present data describing the geophysics and geochemistry of brines from a mud volcano and a stable brine pool in the northern Gulf of Mexico. Geophysical signatures of the environment and temperature profiles through the brines illustrate variable and dynamic fluid flow regimes at both sites. Depth profiles of geochemical constituents varied between the mud volcano and the brine pool and both brines served as sources of energy-rich substrates to the surrounding environment.

2. Methods

2.1. Site characterization

In May 1998, the submarine NR-1 (and her tender M/V CAROLYN CHOUEST) was used to survey two brine-dominated cold seeps in the Gulf of Mexico: site GB425 (27°33.2′ N, 92°32.4′ W; 600 m water depth) and site GC233 (27°43.4′ N, 91°16.8′ W; 640 m water depth) (Fig. 1). The NR-1 was equipped with an EdgeTech X-star chirp system (2–12 kHz subbottom profiler) and a Raytheon LS4096 laser line scanner. The subbottom profiler was used to obtain high-resolution imaging of near-bottom sediment layers while the laser line scanner was used to produce high-resolution, large-area surface images of the seafloor.

2.2. Collection of brine samples

Temperature profiles through the brines and collection of discrete vertical brine samples were obtained during research cruises on board the "RV Seward Johnson II" using the research submersible "Johnson Sea Link II" (Harbor Branch Oceanographic Institute). During expeditions in 1991, 1997 and 1998, temperature profiles through these brine pools were obtained by lowering a SBE19 CTD into each pool using a small winch mounted on the submersible. This equipment was not available for the 2002 expedition.

An instrument called the "brine-trapper" (Fig. 2) was used to collect discrete depth samples of brine during cruises in 1998 and 2002. The brine trapper consisted of an outer PVC shell pierced by a regularly spaced windows and a series of inner delrin plugs connected by a stainless steel rod. Each end of the plugs was fitted with an O-ring bore seal. The spaces between the plugs formed a series of internal compartments, each having a volume of about 200 mL. The compartments were open to the environment when aligned with the windows and closed when the plugs were aligned with the windows. Each sampling compartment was fitted with a pressure-relief valve

and a sampling port (Fig. 2A). On the surface and during descent to the bottom, the compartments were in the open position. On the seafloor, the trapper was lowered vertically into the brine using a hydraulically actuated lever mounted on the side of the submersible (Fig. 2B). The top chamber was visually aligned in the overlying seawater above the brine-seawater interface. Once the trapper was in position, chambers were permitted to equilibrate, and then a hydraulic actuator pulled on the connecting rod to align the plugs with the windows and seal the compartments. The trapper was removed from the brine and positioned horizontally along the side of the submersible for return to the surface.

When the submersible was safely on deck, the brine trapper was removed and sampled. Because of the length (3 m) of the instrument, sampling had to be done on deck and was carried out as quickly as possible in the shade within 30 min of return to the surface. For each chamber, the sampling valve was opened and two samples of the venting gas were collected and transferred to a helium-purged, evacuated serum bottle (20 mL). After collecting gas samples, the overpressure was relieved so that the brine fluids could be collected. Next, a length of argon-purged tubing was attached to the sampling port, the valve was opened, and the fluid from each chamber was transferred into an argon-purged 60-mL syringe. The brine fluid was transferred from the syringe into an argon-purged, clean (3×10% HCl washed and milliQ water rinsed) 500 mL PETG sampling bottle. Then, the headspace of the sampling bottle was purged with argon and bottles were capped and transferred to a 4°C cold room for processing. Sub-samples for geochemical analyses were filtered (0.2 μm Millex syringe-tip filter) before dispensing aliquots into vials for various analyses (see below).

2.3. Geochemistry

The concentration of dissolved hydrocarbons (C_1–C_5) in the venting gas from the compartments of the brine trapper was determined by injecting a 0.25 cc sub-sample into a Shimadzu gas chromatograph equipped with a Hayes-Sep-D column (2 m), which separated C_1-C_5 hydrocarbons as a programmed temperature ramp was applied, and a

flame ionization detector, which quantified sample signals (Joye et al., 2004). Certified standard gas mixtures (10% CH_4 and a C_1–C_5 mix in a balance of He) were used to calibrate the GC signals. Analytical precision was between 1.5 and 4%. Appropriate blanks and internal standards (as noted) were run routinely in the following geochemical analyses and sample concentrations were determined by comparison to a curve generated using certified standards. The carbon isotopic composition of methane was determined using a gas chromatograph coupled to an isotope ratio monitoring mass spectrometer (Popp et al., 1995).

Sub-samples (1.5 mL) for the determination of dissolved anion (sulfate, SO_4^{2-}, and chloride, Cl^-) and cation (magnesium, Mg^{2+}, calcium, Ca^{2+}, sodium, Na^{2+} and potassium, K^+) concentration were acidified using ultrex HNO_3 (100 μL HNO_3 per mL sample). Major ion concentrations were quantified on a Dionex DX5000 ion chromatograph after dilution by either 1:100 (for concentrations >2 mM) or 1:10 (for concentrations <2 mM). For SO_4^{2-} analysis, precision was 1.5% for concentrations >2 mM and 5–7% for <2 mM. Precision for other ions was always better than 1%. Dissolved reduced iron (Fe^{2+}) concentration was determined in an aliquot of the acidified major ion sample using the Ferrozine colorimetric method (Stookey, 1979). Dissolved inorganic carbon concentration was determined using a Shimadzu TOC5000 infrared gas analyzer. Samples for the determination of dissolved nutrients were filter-sterilized and stored at 4°C until analysis on board the ship. Nitrate (NO_3^- = nitrate plus nitrite), phosphate (PO_4^{3-}) and silicate ($H_2SiO_4^{2-}$) concentrations were determined using standard methods on a Lachat 3-channel QuikChem 8000 autoanalyzer. Precision of these analyses was about 2%. Ammonium (NH_4^+) was analyzed immediately on board ship using the indo-phenol colorimetric method (Solaranzo, 1969) with an analytical precision better than 2%.

BGD
2, 637–671, 2005

3. Results

3.1. Geologic and geophysical setting

Brine, gas and/or oil (GB425 only) seepage occurs at both sites. The GC233 environment represents a stable, stratified brine pool whereas the GB425 site represents a well-mixed, mud-volcano type formation where high rates of fluid discharge generates large, episodic temperature fluctuations. Visual observations and temperature records suggest that, on average, fluid flow at GB425 exceeds that at GC233. Laser line scan and subbottom data illustrated the geologic nature of both sites (Figs. 3 and 4). The GC233 site is a small, stable brine pool (190 m^2) situated at a depth of 640 m (MacDonald et al., 1990; Fig. 3). A laser line scan mosaic (Fig. 3A) was geo-rectified in the ER-MAPPER software environment (MacDonald et al., 2000; Sager et al., 2003). The GC233 brine pool is situated on a mound, which is elevated 6 to 8 m above the surrounding seafloor and has a basal diameter of approximately 100 m (Fig. 3). The fluid filling the pool has a salinity of 130 PSU and is supersaturated with gas (Table 1). Added density due to the excess salt maintains the brine as a distinct fluid in the pool but the brine mixes with seawater by molecular and eddy diffusion.

Subbottom records revealed considerable complexity at the site. On the flanks of the mound, indurate layers underlie layers with a weak seismic reflection (Fig. 3C), suggesting surface flows of loosely consolidated material over hardened ground. A narrow dike, raised about 25 cm, formed a rim that surrounds three sides of the pool outside of the mussel bed. The mussels appear as a layer distinct from the brine, which forms a level reflector. Below the brine, sediments are homogeneous and contain a large, irregular reflector near the bottom of the record. The most regular subbottom features were a sequence of layers buried under the present-day mound. Distances between these layers were greatest in the center of the mound and least around the edges. The deepest layer formed a funnel shaped base to the outline of the mound.

Temperature profiles collected in 1991, 1992 and 1998 (Fig. 6A) show an abrupt interface between brine and seawater and a ~1 m thick mixed layer in which the tem-

BGD
2, 637–671, 2005

perature is elevated about 1.5°C above ambient bottom water temperature. Below this, a thermocline extended over ~1.5 m as the temperature increased to about 17°C. Temperature was essentially stable at depths greater than 3 m below the second thermocline. Visually, the mixed layer was clear, although refraction makes it appear darker than seawater. Within and below the thermocline, the brine contained a high concentration of suspended solids (ca. 50% by volume; data not shown). The pH of the upper brine was about 6.4 while the pH of the lower brine was 6.8 (data not shown). Similar temperature profiles over a 7-year period indicate the recent stability of the pool's density structure.

Seepage at GC233 is dominated by brine and free and dissolved gases (MacDonald et al., 1990). Continuous discharge of gas through the brine leads to saturation with dissolved methane, which serves as a source of energy for mussels with methanotrophic symbionts (Nix et al., 1995) that are found along the edges of the pool. Patchy mats of giant sulfur bacteria, such as *Beggiatoa, Thioploca*, and *Thiomargarita*, covered the sediments adjacent to the mussel beds (Larkin et al., 1994; Nikolaus et al., 2003; Kalanetra et al., 2005) (Figs. 5A and 5B). However, some brine sites experience episodic eruptions and are much more dynamic. An example of a more active site is the GB425 mud volcano.

The GB425 site lies on the western edge of the Auger basin (MacDonald et al., 2000; Fig. 4), an intraslope basin that contains economically significant hydrocarbons in the Auger, Cardamom, and Macaroni fields and is bordered to the west by tabular salt bodies (McGee et al., 1993; Sager et al., 2003). The GB425 mud volcano is situated at a small, active diatreme on the southern margin of a flat-topped mound located mid-way along the fault. A tension-leg platform installed at Auger Field is producing from an estimated 100 million barrels of extractable oil (Shew et al., 1993), but large quantities of pressurized fluid have evidently escaped through anticline faults along the flanks of the salt body at the basin margin. Fluids migrating up these faults disturb surface sediments due to the formation of carbonate nodules, oil and gas pockets, and biogenic debris. Sediment cores from the area contained high-molecular weight

hydrocarbon and thermogenic gas hydrate (MacDonald et al., 2000).

Frequent and active venting of brine, free and dissolved gases, and high molecular weight hydrocarbons sustains an expulsion crater from which gas and fluidized mud streams are visible (MacDonald et al., 2000). The sediments adjacent to the south of the diatreme support chemosynthetic mussel communities and mats of free-living giant sulfur bacteria (Figs. 6C and 6D), however, the distribution of mussels and microbial mats is more patchy at GB425 than that at GC233. The GB425 site, which is physically larger than the GC233 pool, supports a higher rate of gas discharge and flows of fluidized muds (MacDonald et al., 2000). The GB425 brine consisted of fine clay suspended in brine with a salinity of about 133 PSU. The suspended sediment load is at least 65% by volume (data not shown). The mud volcano brine pH was about 7.4. A temperature profile through the brine obtained in 1997 showed only slight elevations in brine temperature in comparison to the overlying bottom water. However, in 1998, a maximum temperature of 26.2° C was observed less than 0.5 m below the interface (Fig. 6B). Only a 1 m record was obtained as the CTD hit the bottom of the pool at the location sampled.

3.2. Geochemistry

A comparison of depth profiles of geochemical parameters between the brine pool and mud volcano underscored fundamental differences between the two environments. Our sampling protocol ensured that the uppermost chamber contained seawater from just above the brine-seawater interface, which we used as our zero depth reference; the geochemistry of the seawater sample at both sites was similar. Both brines were gas charged, containing large amounts of primarily methane in gas vented from the chambers (Table 1). At the brine pool, methane accounted for 99.9% of C1-C5 hydrocarbons and the carbon isotopic composition of the methane (δ^{13}C-CH_4) was −66‰. At the mud volcano, methane accounted for 94 to 98% of C1-C5 hydrocarbons and the δ^{13}C-$CH_4$was −60‰.

Both brines contained similar concentrations of Na^+ (∼1800 mM) and Cl^- (2100

mM), little to no SO_4^{2-} (0 to 1 mM), and exhibited a slight decrease in Mg^{2+} concentration with depth into the brine (Fig. 7). In the brine pool, the transition between the overlying seawater and the brine occurred gradually between 30 and 150 cm (Figs. 7A and 7B). In the mud volcano, the transition from overlying seawater to the brine occurred rapidly, with a steep gradient observed between 60 and 90 cm (Figs. 7C and 7D). Calcium concentrations increased with depth in both brines but reached higher concentrations in the mud volcano. Potassium concentration decreased with depth in the brine pool but increased with depth in the mud volcano (Figs. 7B and 7D). Plots of salts versus sodium concentration for the two brines suggested different end-member compositions for the two brines (Fig. 8). A comparison of the geochemistry of the brines described here to other deep-sea brines is provided in Table 2.

Nitrate concentrations were high in the overlying seawater and decreased with depth in the brine (Fig. 9). In the brine pool, NO_3^- versus Cl^- concentration plots showed conservative mixing between the two end-member fluids (data not shown). In the mud volcano, the transition between the seawater and brine was abrupt but a plot of NO_3^- versus Cl^- concentration for 0 to 90 cm samples suggested a possible sink for NO_3^- in the 30 and 60 cm samples (data not shown). Phosphate concentrations doubled from 2 μM in the overlying seawater to 4 μM in the brine. Silicate concentrations increased from 40 μM in the overlying seawater to over 200 μM in the brine (Fig. 9). Ammonium concentrations increased from ~0.5 μM in the overlying seawater to between 12 (brine pool) and 8 (mud volcano) mM at depth in the brine (Fig. 9). Concentrations of reduced iron (Fe^{2+}) were higher at GC233 while concentrations of DIC were higher at GB425 (Fig. 10).

4. Discussion

We used an integrated approach to evaluate the dynamics and biogeochemical signatures of two brine-dominated cold seeps along the continental slope in the Gulf of Mexico. Our data support two major conclusions: 1) Fluid, gas and mud discharge

rates differed between the two sites but both sites were likely sources of methane, ammonium, and in the case of the GB425 brine and oil, to the surrounding environment. Variations in fluid flow rates resulted in different mixing regimes in the two brines and this difference likely contributed to the variations in geochemistry that we observed. 2) While the sodium and chloride content of brines from the brine pool and mud volcano were similar, concentrations of other major ions differed suggesting different sources and/or sinks for dominant ions in the brine fluids.

4.1. Fluid discharge at brine-dominated cold seeps

The present study focused on two brine-dominated seeps in the Gulf of Mexico: the Brine Pool NR1, located in lease block GC233 (MacDonald et al., 1990) and the mud volcano, located in lease block GB425 (MacDonald 1998; MacDonald et al., 2000). At both sites, central pools of fluidized mud and hypersaline brine have core temperatures that are $\geq$10°C warmer than ambient seawater (Fig. 6). While spatio-temporal variation in seepage rates exists at both sites (MacDonald et al., 2000), some degree of seepage, albeit low at times, occurs continuously. The rate of fluid discharge influences the degree of stratification within the central pool of brine and the two sites reflect discrete end-members of brine stratification, as evidenced by the different temperature profiles observed at the two sites (Fig. 6). The GC233 site is a more stable, stratified brine pool whereas GB425 is a well-mixed, mud-volcano type formation in which fluid discharge generates episodic temperature fluctuations in the overlying bottom water (MacDonald et al., 2000).

At GC233, fluid discharge is limited to a sparse stream of small bubbles emanating from the center and northern edge of the pool. Temperature profiles show an abrupt interface between brine and seawater and below this, a ~m-thick mixing zone between the brine and the overlying seawater is apparent. This mixing zone is also apparent in the salt profiles (Fig. 7). The salt diapir beneath the GC233 brine pool lies within 500 m of the seafloor (MacDonald et al., 1990; Reilly et al., 1996). At the GB425 site, strong seismic reflectors at 50 and 150 ms twt beneath the active volcano suggest the

presence of a very shallow salt body (Sager et al., 2003). No such reflectors appear in the 2D lines from GC233 (Sager et al., 2003). The shallow depth of the salt body beneath the GB425 site may contribute to the enhanced fluid flow that is apparent at this site.

The elevation of the GC233 mound, sediment slides and bacterial mats on the down slope (southern) end of the pool, and a raised dike around the upslope (northern) edge of the pool, provide evidence that the pool was excavated by a vigorous discharge of fluid (Fig. 3). The persistence of a mussel community, developed in the present day to a continuous band that completely surrounds the pool on the level margins of the crater (Fig. 3), is strong evidence for conditions that have favored chemosynthetic communities over an extended period of time. The probable age of the larger seep mussels in this population exceeds 100 y (Nix et al., 1995), which suggests that the lifetime of the pool is on the order of hundreds of years. Long-term stability of the level of brine filling the pool is essential because the brine is anoxic in addition to being hypersaline. Therefore, it would be fatal for mussels to be submerged in the brine.

The GB425 site supports a greater rate of gas and fluidized mud discharge (MacDonald et al., 2000). Active fluid expulsion is localized in a 50-m wide, sub-circular crater on the southwestern edge of the summit, which is one of two such vents on the mound (Fig. 4). Fine, fluidized mud overflows the northeastern margin of the crater and moves down the southern flank of the mound. The mud is fluidized in hypersaline brine that is supersaturated with methane (Table 1). Beds of the seep mussel rim the southern edge of the crater (Figs. 5C and 5D). Sampling of this site over the past eight years has documented substantial variations in flow regimes. In 1997, visual observations indicated that gas and oil discharges were minor. In 1998, however, a continual stream of small gas bubbles and drops of oil emanated from the central diatreme, while bursts of larger bubbles, oil drops, and suspended sediment periodically escaped from the surrounding mud; similar high flow conditions were observed during dives conducted in 2002. Such large, continuous eruptions lead to conspicuous sea surface oil slicks that can be mapped easily using Synthetic Aperture Radar (SAR; cf. MacDonald et al.,

BGD
2, 637–671, 2005

2000).

Evidence for discontinuous fluid discharge was apparent in a temperature record obtained from a thermistor suspended at the shallow edge of the mud volcano between 1997 and 1998 (MacDonald et al., 2000). The temperature at the brine-seawater interface fluctuated between 6.9 and 48.2°C, and had an average temperature of 26.1±9.1°C (MacDonald et al., 2000), about 20°C warmer than ambient bottom waters. The temperature changes observed over short time periods (~days) underscored the ephemeral nature of fluid flow at this site (MacDonald et al., 2000). In 1998, the near surface (~0.5 m below the interface) temperature of the GB425 brine was about 15°C warmer than temperatures observed in the GC233 brine. The high temperatures near the seawater interface suggest that the GB425 site supported higher rates of fluid flow than GC233. Mixing in the GB425 brine is driven by increased thermal flux and results in increased gas and oil release from the brine to the surrounding environment. While we cannot presently constrain fluid flow rates at either of these sites, the available data show clearly that the physical regime of these two sites is very different.

4.2. Geochemical signatures of deep-sea brines

Fluid flow at the mud volcano and the brine pool clearly influenced the geochemical signature of both brines as well as the distribution and activity of microorganisms in the brine fluids (Joye et al., in preparation[1]). Both brines were gas-charged, containing a mixture of C1-C5 hydrocarbons that was dominated by methane. Most of the methane fluxing from cold seeps in the Gulf of Mexico is thermogenic (Brooks et al., 1984). The dominance of the gas mixture seeping from the brine sties by methane (>98% CH_4) and the $\delta^{13}C$ of that methane (−66 to −60‰ VPBD) suggested a mixed thermogenic and biogenic source for methane at both sites, with more of a thermogenic signature at the mud volcano (Table 1). At the GC233 brine pool, trace quantities

[1] Joye, S. B., Samarkin, V. S., MacDonald, I. R., Montoya, J. P., and Orcutt, B. N.: A Window into the Deep Biosphere: Microbial Activity in Seafloor Brines, in preparation.

of ethane and propane were observed but butane, iso-butane and pentane were not detectable. In contrast, at the GB425 mud volcano, ethane and propane concentrations were two to three orders of magnitude higher than those observed at GC233 and butane, iso-butane and pentane concentrations were substantial, again suggesting a larger input of thermogenic gas at this site (data not shown). Vigorous gas discharge from the mud volcano created walls of bubbles that emanated along fault tracks for 10's of meters (Joye et al. personal observation and video documentation). The gas plume rising from the mud volcano (visualized using CHIRP sonar, data not shown) reached >200 m above the seafloor (Joye et al., unpublished data). Methane-rich plumes originating from cold seeps, such as those documented in the Gulf of Mexico (Aharon et al., 1992b; MacDonald et al., 2000; MacDonald et al., 2002) are common features along continental margins across the globe (Charlou et al., 2003 and references therein). Seafloor mud volcanoes, in particular, are likely important, but poorly constrained, sources of methane to the overlying water column and potentially to the atmosphere (Milkov, 2000; Dimitrov, 2002). Future studies in the Gulf of Mexico and elsewhere should aim to quantify the role of seafloor mud volcanoes in regional and global methane budgets.

The depth distribution of major ions in the two brines also supported the hypothesis that fluid flow rates are higher at the mud volcano. The seawater-brine mixing zone in the brine pool extended over more than one meter. In contrast, the seawater-brine transition occurred abruptly in the mud volcano, with a small change in salinity observed between 30 and 60 cm and a 3-fold increase in salinity observed between 60 and 90 cm. Sulfate was rapidly depleted to zero within the mud volcano brine but small (<1 mM) concentrations persisted at depth within the brine pool. We propose that low sulfate concentrations at depth in the brine pool were maintained by anaerobic H_2S oxidation using reactive metal (Fe, Mn) oxides as oxidant (Van Cappellen et al., 1998). Sulfate reduction occurs at high rates in the GC233 brine (rates exceed 1 μM d^{-1}, data not shown; Joye et al., in preparation[1]) and Fe^{2+}concentrations are substantial (~90 μM, Fig. 10) while H_2S concentrations are barely detectable (2 μM), suggesting

BGD
2, 637–671, 2005

a potential coupling of iron oxide reduction to H_2S oxidation, which has been observed in the nearby Orca Basin brine (Van Cappellen et al., 1998).

The concentration, depth distribution, and ratio of Mg^{2+}, Ca^{2+} and K^+ to Cl^- were surprisingly variable between the two brines. The concentration of Mg^{2+} was slightly higher in the brine pool (9.8 vs. 8.8 mM, Figs. 7 and 8). However, the Mg/Cl ratio was identical at both sites (0.02) and did not vary with depth, suggesting no net difference in Mg^{2+} sources/sinks between the sites. The slight decrease in Mg^{2+} concentration over depth observed at both sites may result from dolomite or low-magnesium calcite precipitation (Charlou et al., 2003). The low DIC concentrations observed in both brines could result from DIC removal via carbonate precipitation. Calcium concentrations in both brines increased with depth, and this increase was much higher in the mud volcano (5X increase) than in the brine pool (3X increase) (Fig. 7). Likewise, the Ca/Cl ratio increased from about 0.02 (overlying seawater) to 0.6 in the brine pool and 0.10 in the mud volcano, showing a net increase in Ca^{2+} at depth. The increase in Ca^{2+} could reflect the replacement of Ca^{2+} in carbonates by Mg^{2+} or this could reflect differences in the source fluid (see below).

Potassium (K^+) concentrations decreased by a factor of 2 with depth at the brine pool (20 mM in the brine) but increased by a factor of 2 with depth in the mud volcano (90 mM in the brine). Clay mineral reactions at depth below the seafloor may drive the variations in K^+ concentrations we observed. Lower K^+ concentration in the GC233 brine could reflect kaolinization of illite, which removes K^+ from solution at depth (Land and McPherson, 1992). Similarly, K^+ can be enriched in brines by the dissolution or albitization of K^+-rich feldspars (Land and McPherson, 1992). High temperature (~40°C) reactions between the brine fluid and sediments also promote K^+ enrichment in the brine (Charlou et al., 2003). The temperatures observed at mud volcano (brine T>40°C have been documented; MacDonald et al., 2000) suggest that high temperature reactions may contribute to the K^+ enrichment observed at this site.

The differences in salt composition suggests that the two brines either originated from different sources or have reacted differently with sediments during transit from

deep reservoirs. Two major salt depositional events occurred in the Gulf of Mexico, one during the Mesozoic and one in the Cenozoic. Most Mesozoic evaporites in the Gulf of Mexico are Ca-type evaporates while most Cenozoic evaporates are Na-Cl type evaporites (Land and McPherson, 1992). The sodium to chloride ratio (Na/Cl) in both the brines we examined exceeded the Na/Cl ratio (0.82) of seawater (Fig. 8). The Na/Cl ratio in the deeper samples collected from the brine pool was as high as 0.94, suggesting the brine was derived largely from halite dissolution (most likely Cenozoic Na-rich evaporites). In contrast, the most elevated Na/Cl ratio observed in the deeper samples collected from the mud volcano was 0.86, suggesting the brine is not derived primarily from halite dissolution. Dissolution of other evaporitic minerals would increase the Ca^{+}/Cl^{-} and SO_4^{2-}/Cl^{-} ratios but those ratios decreased in the GB425 brine, suggesting the brine was not derived from gypsum or anhydrite dissolution. The most likely explanation for the lower Na/Cl ratio and the brine chemistry observed in the mud volcano is that the brine was derived from residual evaporated seawater that had not reached the halite precipitation stage (Vengosh et al., 1998) and that the brine has reacted significantly with sediments during transit to the surface (Charlou et al., 2003).

Very little data on nutrient concentrations in brines exists. While some data on ammonium or phosphate concentration is available in the literature, few measurements of silicate and nitrate concentrations have been reported. Nutrient distributions in the two brines followed similar trends. Phosphate concentrations were low at both sties (<5μM) and there was little variation in concentration over depth. Silicate concentrations increased significantly in both brines, and the highest concentration was observed at the base of the seawater-brine mixing zone (Fig. 9). Silicate concentration in the brines was 5 times the bottom water concentration, suggesting the brines are an important source of silicate to the bottom water.

In contrast, nitrate concentrations were high (ca. 30 μM) in overlying bottom water but low in the brines. Though the nitrate concentration in both brines was low ($\leq$1 μM, Fig. 9) but measurable, NO_3^{-}/Cl^{-} mixing curves suggested conservative mixing be-

tween the overlying seawater and the brines (data not shown). Though denitrification could occur in the anoxic brines, available data suggest if process occurs, it occurs at low rates (possibly at GB425 but not at GC233), and is not particularly important. Ammonium concentrations in both brines were extremely high (up to 11 mM). Similarly high concentrations of NH_4^+ have been reported from other brines in the Mediterranean (3 mM, Sass et al., 2001; 20 mM, Aloisi et al., 2004; Table 2) but an explanation for these high NH_4^+ concentrations is lacking. We speculate that NH_4^+ associated with clay minerals is desorbed as the brine migrates through the underlying sediments. Loosely bound NH_4^+ represents an important NH_4^+ pool in sediments and the routine method for quantifying this N pool is to use a high ionic strength salt solution (either KCl or NaCl) to desorb the NH_4^+ from the solid phase (Rosenfeld 1979; Mackin and Aller, 1984). The transit of a brine solution through sediments represents a similar, though natural, desorption processes. Because of the high NH_4^+ concentration, the DIN/DIP ratio (=((NO_3^- + NH_4^+)/HPO_4^{2-})) of the brine (>1000 and up to 6000) greatly exceeded that in the bottom water (~40). However, the majority of the brine derived NH_4^+ is consumed, possibly during nitrification, during mixing of the brine with seawater. This impact of this N input in terms of driving DIP limitation of biology in the water column or surficial sediments is not known at present.

5. Conclusions

The two brine systems described here have unique geochemical signatures that result from variations in the source fluid as well as processes, including higher temperature reactions between brines and the sediments as they transit during ascent to the surface. Unlike many of the brines in the Mediterranean (Table 2; Sass et al., 2001; Charlou et al., 2003), the Gulf of Mexico brines have low sulfide and contain little to no sulfate. Enrichment of CH_4 and NH_4^+, in particular, in the brines makes fluid flow from mud volcanoes an important source of energy rich compounds to the surrounding environment. In all likelihood, methanotrophic and nitrifying bacteria in the overlying water

BGD
2, 637–671, 2005

column consume these materials shortly after their release, making mud volcanoes and brine pools important sources of reduced materials that fuel chemoautotrophic processes that are commonly associated with ocean floor cold seeps.

Acknowledgements. We thank members of science parties of the CHEMO 1997, CHEMO 1998 and LExEn 2002 research cruises, the crew of the "R/V Seward Johnson II", and the pilots and crew of the deep submergence vehicle "Johnson Sea Link" for assistance with sample collection. B. Orcutt and M. Erickson assisted with processing and analysis of geochemical samples. A. Pachachy assisted with the design of the brine trapper and processing the geophysical data. This research was supported by the National Science Foundation "Life in Extreme Environments" Program (OCE-0085549), the American Chemical Society (PRF-36834-AC2), and the US Department of the Interior's Minerals Management Service (contract nos. 14-35-0001-30555 and 14-35-0001-31813). The US Department of Energy, the Minerals Management Service, the National Undersea Research Program, and the Georgia Institute of Technology provided financial support for submersible operations.

References

Aharon, P., Graber, E. R., and Roberts, H. H.: Dissolved carbon and d13C anomalies in the water column caused by hydrocarbon seeps on the northwestern Gulf of Mexico slope, Geo-Marine Letters, 12, 33–40, 1992a.

Aharon, P., Roberts, H. H., and Snelling, R.: Submarine venting of brines in the deep Gulf of Mexico; observations and geochemistry, Geology, 20, 483–486, 1992b.

Aloisi, G., Drews, M., Wallmann, K., et al.: Fluid expulsion from the Dvurechenskii mud volcano (Black Sea): Part I. Fluid sources and relevance to Li, B, Sr, I and dissolved inorganic nitrogen cycles, Earth and Planetary Science Letters, 225, 347–363, 2004.

Anschutz, P., Turner, J. S., and Blanc, G.: The development of layering, fluxes through double-diffusive interfaces, and location of hydrothermal sources of brines in the Atlantis II Deep: Red Sea, Journal of Geophysical Research, 103, 27 809–27 819, 1998.

Bouma, A. H. and Bryant, W. R.: Physiographic features of the northern Gulf of Mexico continental slope, Geo-Marine Letters, 14, 252–263, 1994.

Brooks, J. M., Kennicutt, M. C., Fay, R. R., et al.: Thermogenic gas hydrates in the Gulf of Mexico, Science, 223, 696–698, 1984.
Brooks, J. M., Wiesenburg, D. A., Roberts, H. H., et al.: Salt, seeps and symbiosis in the Gulf of Mexico, EOS, Trans. Am. Geophys. Union, 71, 1772–1773, 1990.
Bryant, W. R., Simmons, G. R., and Grim, P. J.: The morphology and evolution of basins on the continental slope, northwest Gulf of Mexico, Transactions – Gulf Coast Association of Geological Societies, 51, 73–82, 1991.
Bryant, W. R., Bryant, J. R., Feeley, M. H., et al.: Physiographic and bathymetric characteristics of the continental slope, northwest Gulf of Mexico, Geo-Marine Letters, 10, 182–199, 1990.
Carson, B. and Screaton, E. J.: Fluid flow in accretionary prisms: Evidence for focused, time-variable discharge, Reviews of Geophysics, 36, 329–351, 1998.
Charlou, J. L., Donval, J. P., Zitter, T., et al.: Evidence of methane venting and geochemsitry of brines on mud volcanoes of the eastern Mediterranean Sea, Deep - Sea Research I, 50, 951–958, 2003.
Cita, M. B.: Anoxic basins of the Mediterranean: An overview, Paleoceanography, 6, 133–141, 1990.
Cita, M. B., Camerlenghi, A., Erba, E., et al.: Discovery of mud diaperism in the Mediterranean Ridge: a preliminary report, Bulletin of the Society of Geology of Italy, 108, 537–543, 1989.
Commeau, R., Paull, C. K., Commeau, J., et al.: Chemistry and mineralogy of pyrite-enriched sediments at a passive margin sulfide brine seep: abyssal Gulf of Mexico, Earth and Planetary Science Letters, 82, 62–74, 1987.
De Lange, G. J. and Brumsack, H.-J.: The occurrence of gas hydrates in Eastern Mediterranean mud dome structures as indicated by pore-water composition, in: Gas Hydrates: Relevance to World Margin Stability and Climate Change, edited by: Henriet, J.-P. and Mienert, J., Geological Society, London, 167–175, 1998.
Dimitrov, L. I.: Mud volcanoes-the most important pathway for degassing deeply buried sediments, Earth Science Reviews, 59, 49–76, 2002.
Eder, W., Schmidt, M., Koch, M., et al.: Prokaryotic phylogenetic diversity and corresponding geochemical data of the brine-seawater interface of the Shaban Deep, Red Sea, Environ. Microbiol., 4, 758–763, 2002.
Ginsburg, G. D., Milkov, A. V., Soloviev, V. A., et al.: Gas hydrate accumulation at the Haakon Mosby mud volcano, Geo-Marine Letters, 19, 57–67, 1999.
Henry, P., Le Pichon, X., Lallemant, S., et al.: Fluid flow in and around a mud volcano field

seaward of the Barbados accretionary wedge: Results from Manon cruise, Journal of Geophysical Research, 101, 20 297-20 324, 1996.
Humphris, C. C.: Salt movement in continental slope, northern Gulf of Mexico, AAPG Bulletin, 63, 782–798, 1979.
Joye, S. B., Boetius, A., Orcutt, B. N., Montoya, J. P., Schulz, H. N., Erickson, M. J., and Lugo, S. K.: The anaerobic oxidation of methane and sulfate reduction in sediments from Gulf of Mexico cold seeps, Chemical Geology, 205, 219–238, 2004.
Kalanetra, K., Joye, S. B., Sunseri, N. R., et al.: Novel, large, vacuolate, nitrate-accumulating sulfur bacteria discovered in the Gulf of Mexico reproduce by reductive division in three dimensions, Environmental Microbiology, in press, 2005.
Kennicutt II, M. C., Brooks, J. M., and Denous, G. J.: Leakage of deep, reservoired petroleum to the near surface on the Gulf of Mexico continental slope, Mar. Chem., 24, 39–59, 1988a.
Kennicutt II, M. C., Brooks, J. M., Bidigare, R. R., et al.: Gulf of Mexico hydrocarbon seep communities-I: Regional distribution of hydrocarbon seepage and associated fauna., Deep-Sea Research I, 35A, 1639–1651, 1988b.
Lance, S., Henry, P., Le Pichon, X., et al.: Submersible study of mud volcanoes seaward of the Barbados accretionary wedge: sedimentology, structure and rheology, Marine Geology, 145, 255–292, 1998.
Land, L. S. and Macpherson, G. L.: Origin of Saline Formation Waters, Cenozoic Section, Gulf of Mexico Sedimentary Basin, AAPG Bulletin, 76, 1344–1362, 1992.
Langseth, M. G., Westbrook, G. H., and Hobart, A.: Geophysical survey of a mud volcano seaward of the Barbados Ridge complex, Journal of Geophysical Research, 93, 1049–1061, 1988.
Larkin, J., Aharon, P., and Henk, M. C.: Beggiatoa in microbial mats at hydrocarbon vents in the Gulf of Mexico and warm mineral springs, Florida, Geo-Marine Letters, 14, 97–103, 1994.
Limonov, A. F., Woodside, J., Cita, M. B., et al.: The Mediterranean Ridge and related mud diaperism: a background, Marine Geology, 132, 7–19, 1996.
MacDonald, I. R.: Natural Oil Spills, Scientific American, 279, 51–66, 1998.
MacDonald, I. R., Reilly, J. F., Guinasso, J. N. L., et al.: Chemosynthetic mussels at a brine-filled pockmark in the northern Gulf of Mexico, Science, 248, 1096–1099, 1990.
MacDonald, I. R., Buthman, D., Sager, W. W., et al.: Pulsed oil discharge from a mud volcano, Geology, 28, 907–910, 2000.
Macgregor, D. S.: Relationship between Seepage, tectonics and subsurface petroleum re-

serves., Marine and Petroleum Geology, 10, 606–619, 1983.
McGee, D. T., Bilinski, P. W., Gary, P. S., et al.: Geologic models and reservoir geometries of Auger Field, deepwater Gulf of Mexico, in:Submarine fans and turbidite systems – sequence stratigraphy, reservoir architecture, and production characteristics, edited by: Weimer, P., Bouma, A. H., and Perkins, B. F., SEPM, 233–244, 1993.
Mackin, J. E. and Aller, R. C.: Ammonium adsorption in marine sediments, Limnol. Oceanogr., 29, 250–257, 1984.
MEDINAUT/MEDINETH, S. S. P.: Linking Mediterranean Brine Pools and Mud Volcanism, EOS, 81, 625, 2000.
Milkov, A. V.: Worldwide distribution of submarine mud volcanoes and associated gas hydrates, Marine Geology, 167, 29–42, 2000.
Nikolaus, R., Ammerman, J. W., and MacDonald, I. R.: Distinct pigmentation and trophic modes in Beggiatoa from hydrocarbon seeps in the Gulf of Mexico, Aquatic Microbial Ecology, 32, 85–93, 2003.
Nix, E. R., Fisher, C. R., Vodenichar, J., et al.: Physiological ecology of a mussel with methanotrophic endosymbionts at three hydrocarbon seep sites in the Gulf of Mexico., Mar. Biol., 122, 605–617, 1995.
Neurauter, T. W. and Roberts, H. H.: Three generations of mud volcanoes on the Louisiana continental slope, Geo-Marine Letters, 14, 120–125, 1994.
Neurauter, T. W. and Bryant, W. R.: Seismic expression of sedimentary volcanism on the continental slope, Northern Gulf of Mexico., Geo-Marine Letters, 10, 1990.
Pindell, J.: Alleghenian reconstruction and subsequent evolution of the Gulf of Mexico, Bahamas and proto-Caribbean Sea, Tectonics, 4, 1–39, 1985.
Popp, B. N., Sansone, F. J., Rust, T. M., et al.: Determination of concentration and carbon isotopic composition of dissolved methane in sediments and near shore waters, Analytical Chemistry, 67, 405–411, 1995.
Reilly, J. F., MacDonald, I. R., Biegert, E. K., et al.: Geologic controls on the distribution of chemosynthetic communities in the Gulf of Mexico, in: Hydrocarbon migration and its near-surface expression, edited by: Schumacher, D. and Abrams, M. A., Amer. Assoc. Petrol. Geol., Tulsa OK, 38–61, 1996.
Roberts, H. H. and Carney, R. S.: Evidence of episodic fluid, gas, and sediment venting on the northern Gulf of Mexico continental slope, Economic Geology, 92, 863–879, 1997.
Rosenfeld, J. K.: Ammonium absorption in nearshore anoxic sediments, Limnol. Oceanogr.,

24, 356–364, 1979.
Sager, W. W., MacDonald, I. R., and Hou, R. S.: Geophysical signatures of mud mounds at hydrocarbon seeps on the Louisiana continental slope, northern Gulf of Mexico, Marine Geology, 198, 97–132, 2003.
Sass, A. M., Aass, H., Coolen, M. J. L., et al.: Microbial Communities in the Chemocline of a Hypersaline Deep-Sea Basin (Urania Basin, Mediterranean Sea), Applied and Environmental Microbiology, 67, 5392–5402, 2001.
Schmidt, M., Botz, R., Faber, E., et al.: High-resolution methane profiles across anoxic brine-seawater boundaries in the Atlantis-II, Discovery, and Kebrit deeps (Red Sea), Chemical Geology, 200, 359–376, 2003.
Sheu, D. D.: The Anoxic Orca Basin (Gulf of Mexico): Geochemistry of Brines and Sediments, Reviews in Aquatic Science, 2, 491–507, 1990.
Shew, R. D., Rollins, D. R., Tiller, G. M., et al.: Characterization and modeling of thin bedded turbidite deposits from the Gulf of Mexico using detailed subsurface and analog data, In: Submarine fans and turbidite systems – sequence stratigraphy, reservoir architecture, and production characteristics, edited by: Weimer, P., Bouma, A. H., and Perkins, B. F., SEPM, 327–334, 1993.
Shokes, R. F., Trabant, P. K., Presley, B. J., et al.: Anoxic, Hypersaline Basin in the Northern Gulf of Mexico, Science, 196, 1443–1446, 1977.
Solaranzo, L.: Determination of ammonia in natural waters by the phenol hypochlorite method, Limnology and Oceanography, 1969.
Stookey, L. L.: Ferrozine – A new spectrophotometric reagent for iron, Analy. Chem., 42, 779–781, 1970.
Van Cappellen, P., Viollier, E., Roychoudhury, A., et al.: Biogeochemical Cycles of Manganese and Iron at the Oxic-Anoxic Transition of a Stratified Marine Basin (Orca Basin, Gulf of Mexico), Environmental Science and Technology, 32, 2931–2939, 1998.
Vengosh, A., de Lange, G. J., Gert, J., et al.: Boron isotope and geochemical evidence for the origin of Urania and Bannock brines at the eastern Mediterranean: effect of water-rock interactions, Geochimica et Cosmochimica Acta, 62, 3221–3228, 1998.
Worrall, D. M. and Snelson, S.: Evolution of the northern Gulf of Mexico, with emphasis on Cenozoic growth faulting and the role of salt, in: Decade of North American Geology, edited by: Bally, A. and Palmer, A., Geological Society of America, Boulder, CO, 97–138, 1989.

Table 1. Dissolved methane concentration in parts per million (ppm) and % of total hydrocarbons as methane (in parenthesis) over depth in the brine pool and mud volcano in 1998 and 2002 (n. d. = no data, chambers were too over-pressured for sample collection; * leakage in the chamber during ascent or dilution during sample collection).

Site/Date:	GC233 1998	GC233 2002	GB425 1998	GB425 2002
Depth (cm)	CH_4 ppm (%)	CH_4 ppm (%)	CH_4 ppm (%)	CH_4 ppm (%)
0	765385 (99.9)	8151 (99.9)	n. d.	151440 (97.1)
30	623885 (99.9)	135996 (99.9)	n. d.	539242 (96.7)
60	315908 (99.9)	599541 (99.9)	n. d.	1033369 (96.4)
90	806065 (99.9)	563692 (99.8)	n. d.	951999 (95.2)
120	451206 (99.9)	867947 (99.9)	n. d.	943837 (96.4)
150	944533 (99.9)	817883 (99.9)	n. d.	1020328 (97.6)
180	999515 (99.9)	1012613 (99.9)	916588 (98.3)	917553 (96.2)
210	979935 (99.9)	982982 (99.9)	775103 (98.3)	*521317 (94.1)
240	992897 (99.9)	918422 (99.8)	868131 (98.3)	927599 (96.8)
270	784305 (99.9)	*354070 (98)	n. d.	n. d.

BGD
2, 637–671, 2005

Table 2. Geochemical composition of the GC233 and GB425 brines and other brines from the Gulf of Mexico, Mediterranean, Black Sea and Red Sea. Salinity =‰; all concentrations in mM except Fe^{2+} which is in μM. N.D. denotes "no data". [a] Brine basin or pool, [b] Gulf of Mexico, [c] Mediterranean, [d] Mud Volcano, [e] brine-seawater interface, [f] Black Sea, [g] Red Sea, two stations reported, 3 and 12, [h] Red Sea, estimated from chloride concentration.

Site ID	Salinity	$[Cl^-]$	$[Na^+]$	$[K^+]$	$[Ca^{2+}]$	$[Mg^{2+}]$	$[SO_4^{2-}]$	$[H_2S]$	$[Fe^{2+}]$	$[NH_4^+]$	Reference
GC233	121	2,092	1,751	22	36	9.7	<1	0.002	92	11	This study
GB425	130	2,114	1,790	89	59	8.7	<1	0.004	24	7.6	This study
Bottom water [b]	34	564	462	43	11	11	29	~0	~0	0.1	This study
Orca Basin [a,b]	258	5,000	N. D.	N. D.	32	N. D.	47	0.6	N. D.	0.5	Shokes et al. (1977)
Orca Basin [a,b]	250	4,450	4,240	17.2	29	42.4	20	0.025	30	0.5	Van Cappellen et al. (1998)
Urania Basin [a,c]	200	2,830	N. D.	N. D.	34	N. D.	85	8.6-11	N. D.	N. D.	Sass et al. (2001)
Libeccio Basin [a,c]	321	5,333	N. D.	N. D.	21	N. D.	99	1.7	N. D.	3	Sass et al. (2001)
Tyro Basin [a,c]	N. D.	5,350	N. D.	N. D.	34	N. D.	49	2.1	N. D.	1.2	Sass et al. (2001)
Napoli [c,d]	82	1,380	1,347	8.1	8.4	33.9	28.4	3.5	N. D.	N. D.	Charlou et al. (2003)
Nadir [c,d]	120	1,979	1,884	7.2	22.2	27.9	37.8	5.8	N. D.	N. D.	Charlou et al. (2003)
Urania [c,d,e]	70	1,075	922	26.6	16.8	82.3	44.7	1.6	N. D.	N. D.	Charlou et al. (2003)
Bottom water [c]	35	600	492	11.2	11	56	31	0	N. D.	N. D.	Charlou et al. (2003)
Dvurenchenskii [d,e,f]	50	835	730	4.3	30	18.3	0	0	N. D.	20	Aloisi et al. (2004)
Shaban Deep #3 [a,g]	242	4,358	4,408	44	20	77	N. D.	N. D.	122	N. D.	Eder et al. (2002)
Shaban Deep #12 [a,g]	220	4,361	3,953	39	19	74	N. D.	N. D.	108	N. D.	Eder et al. (2002)
Atlantis-II [a,h]	126	2,000	N. D.	N. D.	N. D.	N. D.	0	0	0	N. D.	Schmidt et al. (2003)
Discovery [a,h]	252	4,000	N. D.	N. D.	N. D.	N. D.	0	0	0	N. D.	Schmidt et al. (2003)
Kebrit [a,h]	252	4,000	N. D.	N. D.	N. D.	N. D.	30	0.4	0	N. D.	Schmidt et al. (2003)

BGD
2, 637–671, 2005

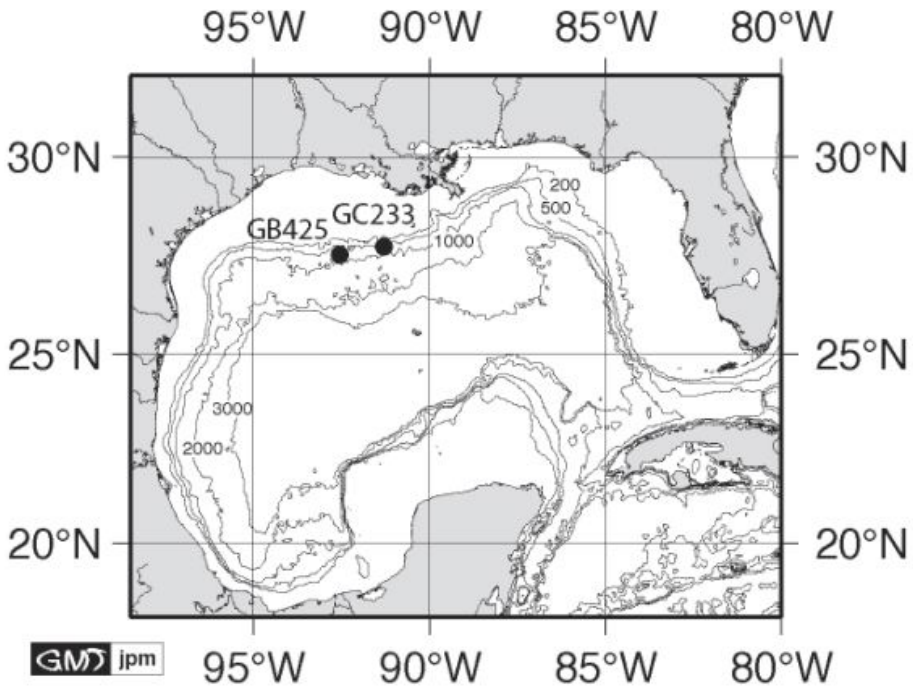

Fig. 1. Map showing the location of the study sites.

BGD
2, 637–671, 2005

Geophysics and geochemistry of seafloor brines

S. B. Joye et al.

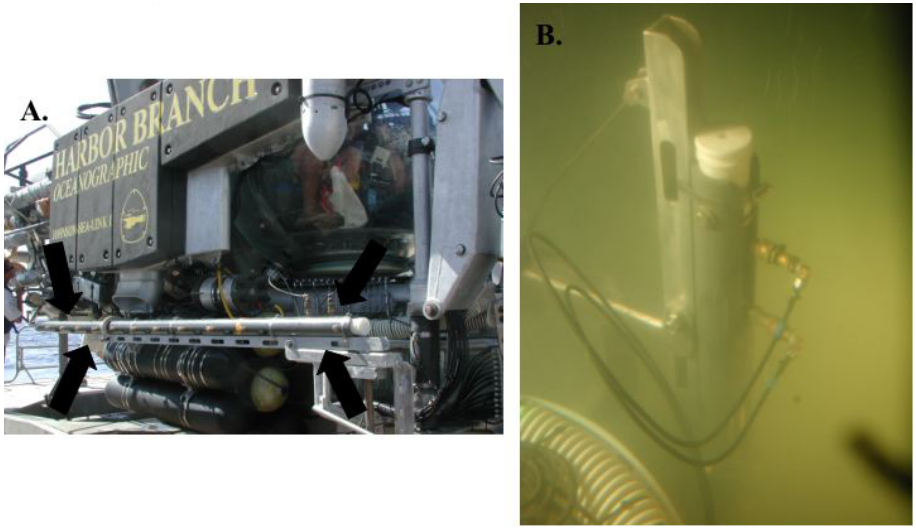

Fig. 2. Photos of the brine trapper used to collect 3-m vertical profiles in deep-sea brines. **(A)** The brine trapper was positioned along the side of the Johnson Sea Link (note black arrows) and was lowered vertically into the brine to collect a profile from the overlying seawater into the core of the brine **(B)**.

BGD
2, 637–671, 2005

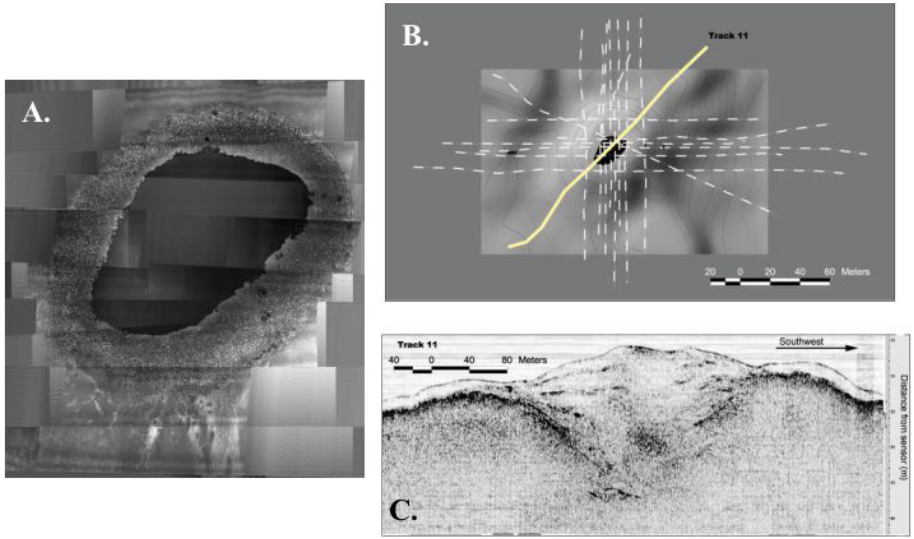

Fig. 3. Laser line scan mosaic and subbottom profile for the GC233 brine pool. **(A)** Laser-line scan mosaic showing the surface of the brine pool and the surrounding rim of mussels. **(B)** Plan of site showing trackline. **(C)** Subbottom record from Track 11 taken along southwest to northeast track. Water depth of submarine was held constant (within <1 m) along trackline, so the bottom profile is accurate.

BGD
2, 637–671, 2005

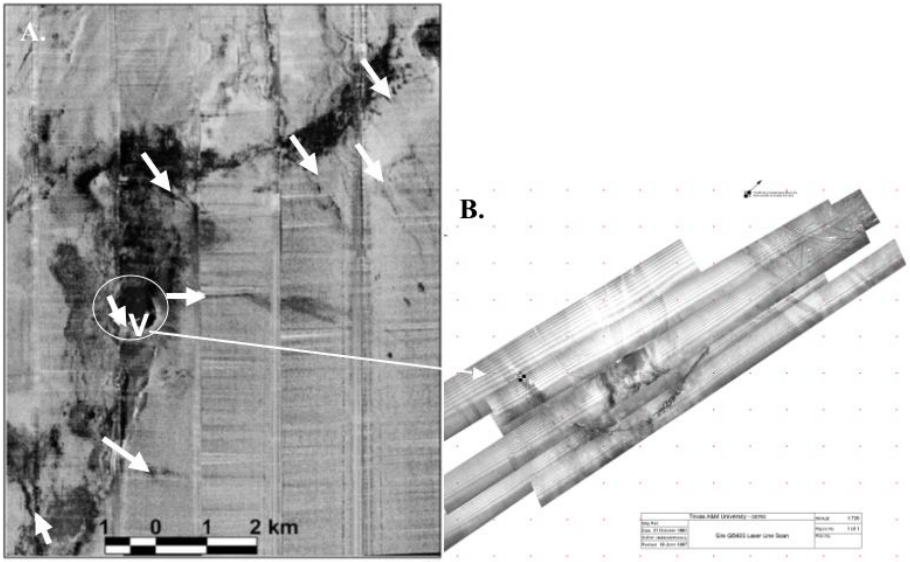

Fig. 4. (A) Side scan mosaic of the GB425 site (adapted from MacDonald et al., 2000). The white arrows on the side-scan mosaic denote major mud vents and the mud volcano is the large pool in the center right noted by "V" and the white circle. **(B)** Laser line scan mosaic of southern rim of the mud-filled crater, showing location of M1 sampling station (grid points are at 10 m centers). Mussel beds are restricted to southwestern (upslope) end of pool.

BGD
2, 637–671, 2005

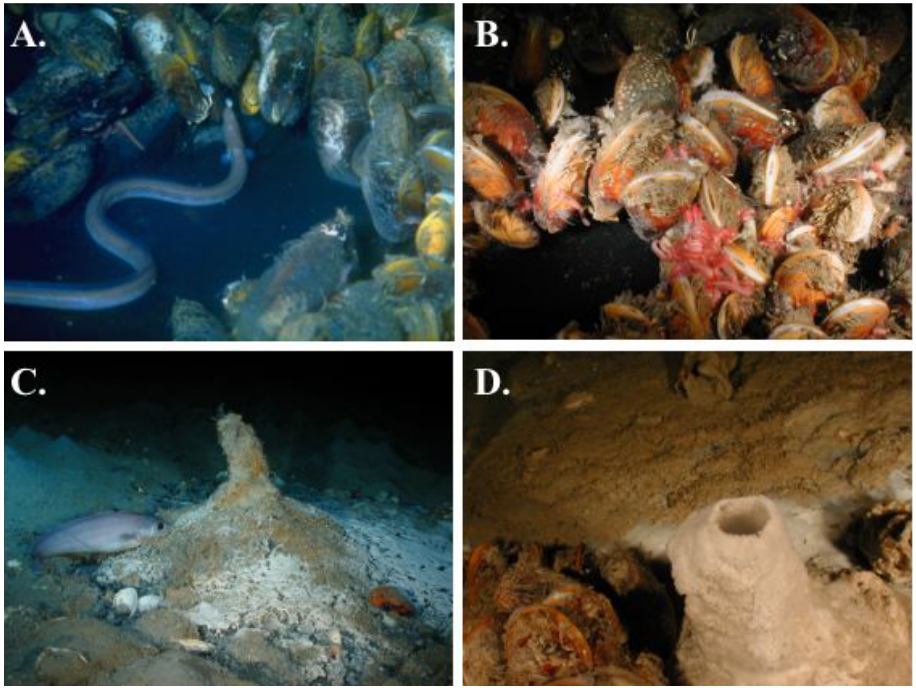

Fig. 5. Images showing bottom features near the GC233 brine pool **(A), (B)** and the GB425 mud volcano **(C), (D)**. A ring of mussels surrounds the GC233 brine pool and eels frequently skim the brine surface (A). Numerous associated fauna cohabitate the mussel bed, such as a variety of amphipods, crabs and polychaete worms (B). White bacterial mats (C) are abundant along the edge of the mud volcano as are barite chimneys (D).

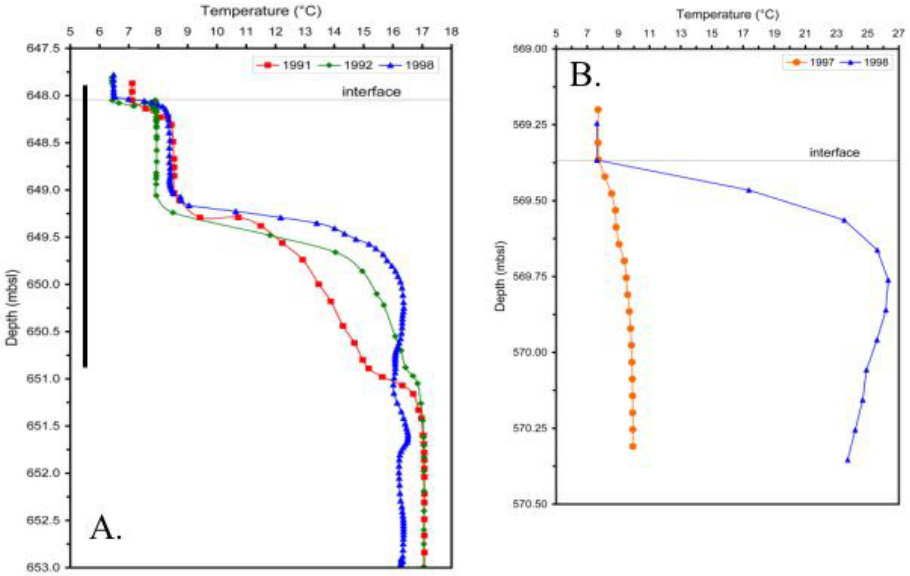

Fig. 6. Temperature profiles from GC233 brine pool **(A)** and the GB425 mud volcano **(B)** collected between 1991 and 1998. Dotted lines mark seawater-brine interfaces. Note the difference in scale between the depth axis on the two panels. The solid horizontal line in panel (A) notes the approximate sampling range of the brine trapper.

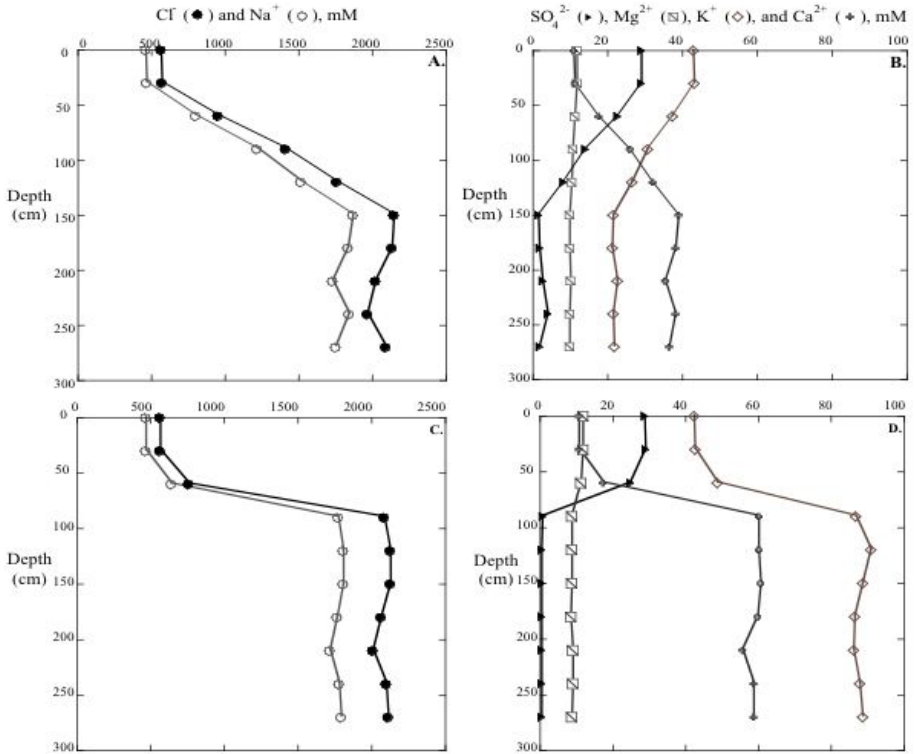

Fig. 7. Depth profiles of major ion concentration in the GC233 brine pool **(A), (B)** and in the GB425 mud volcano **(C), (D)**.

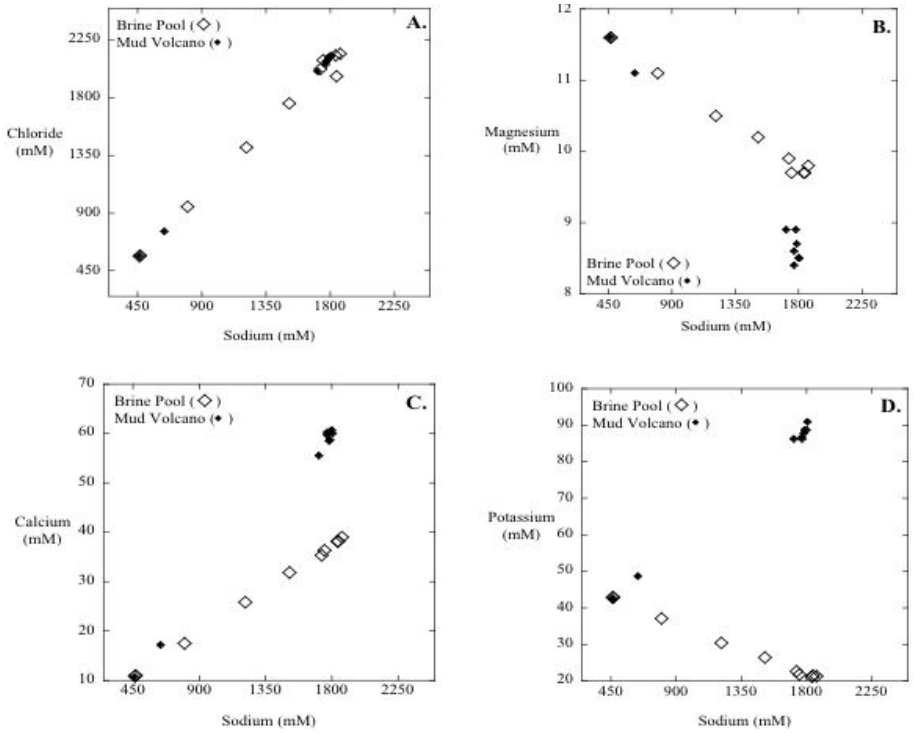

Fig. 8. Plots of chloride **(A)**, magnesium **(B)**, calcium **(C)** and potassium **(D)** versus sodium for the GC233 brine pool and GB425 mud volcano.

BGD
2, 637–671, 2005

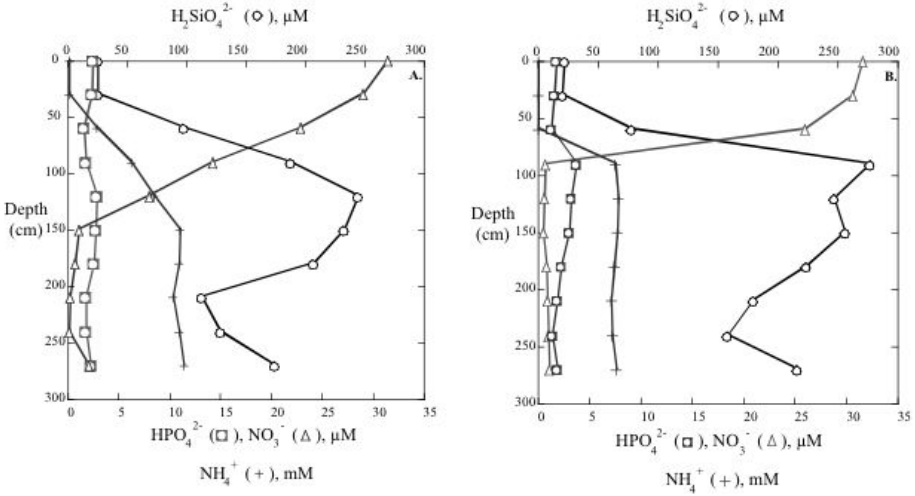

Fig. 9. Depth profiles of nutrient ($H_2SiO_4^{2-}$, NO_3^-, HPO_4^{2-}, and NH_4^+) concentrations in the GC233 brine pool **(A)** and the GB425 mud volcano **(B)**.

BGD
2, 637–671, 2005

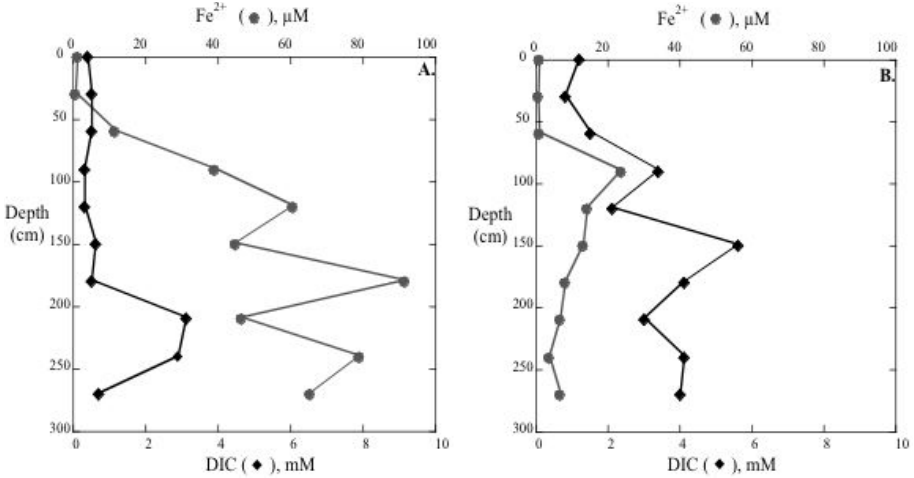

Fig. 10. Concentrations of reduced iron (Fe^{2+}) and dissolved inorganic carbon (DIC) in the GC233 brine pool **(A)** and the GB425 mud volcano **(B)**.